

$t\bar{t}$ production rates at the Fermilab Tevatron and the CERN LHC in top-color-assisted multiscale technicolor models

Chong-Xing Yue,^{1,2} Hong-Yi Zhou,^{1,3} Yu-Ping Kuang,^{1,3} and Gong-Ru Lu^{1,2}

¹China Center of Advanced Science and Technology (World Laboratory), P. O. Box 8730, Beijing 100080, China

²Physics Department, Henan Normal University, Xin Xiang, Henan 453002, China

³Institute of Modern Physics, Tsinghua University, Beijing 100084, China*

(Received 15 August 1996)

We study the contributions of the neutral pseudo Goldstone bosons (technipions and top pions) to the $t\bar{t}$ production cross sections at the Fermilab Tevatron and the CERN LHC in top-color-assisted multiscale technicolor (TOPCMTC) models via the gluon-gluon fusion process from the loop-level couplings between the pseudo Goldstone bosons and the gluons. The MRS set A' parton distributions are used in the calculation. It is shown that the new CDF datum on the $t\bar{t}$ production cross section gives constraints on the parameters in the TOPCMTC models. Models with a large portion of technicolor contributed top-quark mass are disfavored. With reasonable values of the parameters in TOPCMTC models, the cross section at the Tevatron is larger than that predicted by the standard model, and is consistent with the new CDF data. The enhancement of the cross section and the resonance peaks at the LHC are more significant, so that it is testable in future experiments. [S0556-2821(97)03507-8]

PACS number(s): 12.60.Nz, 13.87.Ce, 14.65.Ha

I. INTRODUCTION

Among the yet discovered fermions, the top quark has the strongest coupling to the electroweak symmetry breaking (EWSB) sector, so that processes with top quarks are good for probing the EWSB mechanism. Experimental measurements of the top-quark mass m_t and the $t\bar{t}$ production cross section $\sigma_{t\bar{t}}$ at the Fermilab Tevatron have been improving. In the new 1996 Collider Detector at Fermilab (CDF) data [1], $m_t = 175.6 \pm 5.7(\text{stat}) \pm 7.1(\text{syst})$ GeV and $\sigma_{t\bar{t}} = 7.5_{-1.6}^{+1.9}$ pb, the error bars are well reduced relative to the 1995 data by the CDF and D0 Collaborations¹ [2]. The above experimental value of $\sigma_{t\bar{t}}$ is slightly larger than the standard model (SM) predicted value (taking into account of resummation of soft gluon contributions) which is around 5 pb [3]. Of course, one should wait for further improved data to see whether this really means something. But as the study of the EWSB mechanism, it is interesting to study the $t\bar{t}$ production cross section in EWSB mechanisms other than the SM Higgs sector, and see if the present experimental data can give constraints on the parameters in the EWSB models.

Technicolor (TC) [4] is an interesting idea for naturally breaking the electroweak gauge symmetry to give rise to the weak boson masses. It is one of the important candidates for the mechanism of electroweak symmetry breaking. Introducing extended technicolor (ETC) [5] provides the possibility of generating the masses of ordinary quarks and leptons. The original ETC models suffer from the problem of predicting too large flavor-changing neutral currents. It has been shown, however, that this problem can be solved in walking technicolor (WTC) theories [6]. The electroweak parameter S in WTC models is smaller than that in the simple QCD-like ETC models and its deviation from the experimental central

value may fall within current experimental bounds [7]. To explain the large hierarchy of the quark masses, multiscale WTC (MWTC) model was further proposed [8]. However, even in this model, it is difficult to generate such a large top-quark mass as what is measured at the Tevatron [1] without exceeding the experimental constraint on the electroweak parameter T [9] even with ‘‘strong’’ ETC [10]. In addition, this model generates too large corrections to the $Z \rightarrow b\bar{b}$ branching ratio R_b compared with the data from the CERN e^+e^- collider LEP [11] due to the smallness of the decay constant F_Q . A consistent value of R_b can be obtained² [12] by combining this model with the top-color interactions for the third generation quarks [14] at the energy scale of about 1 TeV. Similar to QCD, the above-mentioned top-color-assisted multiscale technicolor (TOPCMTC) theory predicts certain pseudo Goldstone bosons (PGB’s) including technipions and top pions [8,15–17] which can be the characteristics of this theory.

In the SM, $t\bar{t}$ production at the Tevatron energy is dominated by the subprocess $q\bar{q} \rightarrow t\bar{t}$ [3]. However, in a recent interesting paper, Eichten and Lane [18] showed that, in TC theories, color-octet technipions Π^{0a} could make important contributions to $t\bar{t}$ production at the Tevatron via the gluon-gluon fusion subprocess $gg \rightarrow \Pi^{0a} \rightarrow t\bar{t}$ due to the large triangle-loop gluon-gluon-PGB coupling [cf. Fig. 1(a)], and such PGB’s could be tested by measuring the differential cross section. The contribution of color-octet technirhos to the $t\bar{t}$ production has been considered in Ref. [19]. For a realistic TC model, the masses of technirho are around 1 TeV, and the technirho contribution to $t\bar{t}g$ production is negligibly small as can be inferred from Ref. [19]. PGB loop corrections to $q\bar{q} \rightarrow t\bar{t}$ at the Tevatron are also found to be

*Mailing address.

¹The 1996 D0 data still contain rather large error bars.

²It has been shown that ETC models without exact custodial symmetry may give rise to consistent values of R_b [13], but such models may make the electroweak parameter T too large.

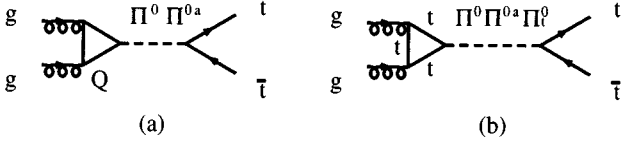


FIG. 1. Feynman diagrams for the TOPCMTC contributions to the $t\bar{t}$ productions at the Tevatron and the LHC. (a). Techniquark loop contributions. (b). Top-quark loop contributions.

within a few percent when Π^{0a} masses are greater than 400 GeV [20]. Considering the total $t\bar{t}$ production cross section, the color-singlet technipion Π^0 also contributes. Furthermore, apart from the technifermion-loop contributions considered in Ref. [18] [Fig. 1(a)], the isospin-singlet PGB's Π^{0a} and Π^0 can also couple to the gluons through the top-quark triangle loop [21], and make contributions shown in Fig. 1(b). In the TOPCMTC theory, the top pion Π_t^0 , as an isospin triplet, can couple to the gluons through the top-quark triangle loop in an isospin-violating way similar to the coupling of π^0 to the gluons in the Gross-Treiman-Wilczek formula [22], and the large isospin violation $(m_t - m_b)/(m_t + m_b) \approx 1$ makes its contribution to the $t\bar{t}$ production cross section important as well [cf. Fig. 1(b)]. In this paper we study all these contributions to the production cross section of the subprocess $gg \rightarrow t\bar{t}$, and use the Martin-Roberts-Stirling (MRS) set A' parton distributions [23] to calculate the cross sections at both the Tevatron and the CERN Large Hadron Collider (LHC). The results of the total production cross sections show that, with these contributions, the cross section at the Tevatron is consistent with the new CDF datum for a certain range of the parameters, and the new CDF datum does give constraints on the parameters in TOPCMTC models. The cross section at the 14 TeV LHC is significantly larger than the SM prediction. The results of the differential cross sections show clear resonances of the PGB Π^{0a} if its mass is in the reasonable range 400–500 GeV. Therefore, this kind of model can be clearly tested by future experiments.

This paper is organized as follows. Section II is devoted to the description of the model and the calculation of the $gg \rightarrow t\bar{t}$ amplitude contributed by the PGB's Π^{0a} , Π^0 , and Π_t^0 . In Sec. III, we present the numerical results of the total contributions of Π^{0a} , Π^0 , and Π_t^0 to the $t\bar{t}$ production cross sections at the Tevatron and the LHC in TOPCMTC models considering all fermion loops in Figs. 1(a) and 1(b). The conclusions are given in Sec. IV.

II. $gg \rightarrow t\bar{t}$ AMPLITUDE CONTRIBUTED BY Π^{0a} , Π^0 , AND Π_t^0

In this paper, we consider a TOPCMTC model in which the simple multiscale technicolor model studied in Refs. [15,18] is assisted with topcolor interaction for the third generation [16]. The model contains one doublet of color-singlet technifermions, ψ , belonging to a higher dimensional representation of $SU(N_{TC})$. It is responsible for most of the electroweak symmetry breaking with the typical decay constant $F_\psi = 220\text{--}235$ GeV of $\bar{\psi}\psi$. The light-scale technifermions are $SU(2)_L$ doublets of techniquarks Q and technileptons L which belong to the fundamental representation of SU

(N_{TC}). These fermions develop condensates at a much lower energy scale than that of the ψ . The top-color sector of this model is the same as in the usual top-color-assisted technicolor theory [16]. In this simple TOPCMTC theory, there are a lot of PGB's. What are relevant to the $t\bar{t}$ production process are the neutral technipions Π^{0a} and Π^0 , and the neutral top pion Π_t^0 . In the MWTC sector, the masses of Π^{0a} and Π^0 have been estimated to be $M_{\Pi^{0a}} \approx 200\text{--}600$ GeV and $M_{\Pi^0} \approx 100\text{--}300$ GeV, and the decay constants are $F = F_Q = F_L \approx 30\text{--}50$ GeV [8]. In the top-color sector, if the top-color scale is of the order of 1 TeV, the mass of Π_t^0 is around 200 GeV and its decay constant is $F_t \approx 50$ GeV [16]. Since these PGB masses are not far from the $t\bar{t}$ threshold and F and F_t are all small, they may give important contributions to the $t\bar{t}$ production rates. In this section, we give the formulas for calculating the production amplitudes $gg \rightarrow \Pi^{0a} \rightarrow t\bar{t}$, $gg \rightarrow \Pi^0 \rightarrow t\bar{t}$, and $gg \rightarrow \Pi_t^0 \rightarrow t\bar{t}$ shown in Fig. 1(a) and Fig. 1(b). These concern the couplings of the PGB's to fermions and to gluons, and the PGB propagators.

In the TOPCMTC theory, the top-quark masses m_t comes from both the top-quark condensate and the ETC sector. It can be made that the large m_t is mainly contributed by the top-quark condensate, so that the ETC-contributed top-quark mass m_t' is very small. For reasonable values of the parameters, $m_t' \sim 5\text{--}20$ GeV [16,24].

We first consider the couplings of the PGB's to $t\bar{t}$. At the relevant energy scale, the PGB's can be described by local fields. In the MWTC theory, the couplings of technipions to fermions are induced by ETC interactions and hence are model dependent. However, it has been generally argued that the couplings of the PGB's to the quark q and antiquark \bar{q} are proportional to m_q'/F [15,17,25], where m_q' is the part of the quark mass acquired from the ETC. (For lighter quarks other than the top quark, m_q' is simply m_q .) The PGB- $q\bar{q}$ vertices are of the forms [17,18]

$$\frac{C_q m_q'}{\sqrt{2}F} \Pi^0 (\bar{q} \gamma^5 q), \quad \frac{C_q m_q'}{F} \Pi^{0a} \left(\bar{q} \gamma^5 \frac{\lambda^a}{2} q \right), \quad (1)$$

where λ^a is the Gell-Mann matrix of the color group and C_q is a model-dependent coupling constant which is expected to be typically of order 1 [15,17,25]. In the top-color sector, by a similar argument, we can obtain the interactions of the top pions with the top quark by replacing m_q' by $m_t - m_t'$, and F by F_t in Eq. (1): i.e., [16],

$$\frac{m_t - m_t'}{\sqrt{2}F_t} \left[\bar{t} \gamma_5 t \Pi_t^0 + \frac{i}{\sqrt{2}} \bar{t} (1 - \gamma_5) b \Pi^+ + \frac{i}{\sqrt{2}} \bar{b} (1 + \gamma_5) t \Pi^- \right]. \quad (2)$$

Next we consider the couplings of the PGB's to the gluons. Consider a general formula for the coupling of a PGB to two gauge fields B_1^μ and B_2^ν . As far as the PGB's are described by local fields, the triangle fermion loops coupling the PGB's to B_1 and B_2 can be evaluated from the Adler-Bell-Jackiw anomaly [26]. The general form of the effective PGB- B_1 - B_2 interaction is [27,17]

$$\frac{1}{(1 + \delta_{B_1 B_2})} \left(\frac{S_{\Pi B_1 B_2}}{4\pi^2 F} \right) \Pi \epsilon_{\mu\nu\lambda\rho} (\partial^\mu B_1^\nu) (\partial^\lambda B_2^\rho), \quad (3)$$

TABLE I. $t\bar{t}$ production cross section $\sigma(gg \rightarrow \Pi^{0(a)}(\Pi^0, \Pi_t^0) \rightarrow t\bar{t})$ at the $\sqrt{s}=1800$ GeV Tevatron in the top-color-assisted multiscale walking technicolor model with $m_{\Pi^0}=150$ GeV. $\Delta\sigma^{(i)}$ is the TOPCMTC correction to the tree-level SM cross section and $\sigma_{t\bar{t}}^{(i)}$ is the total cross section, where $i=1,2,3$ corresponds to $m_t'=5$ GeV, 15 GeV, and 20 GeV, respectively. A factor of 1.6 of QCD corrections has been taken into account.

$M_{\Pi_t^0}$ (GeV)	$M_{\Pi^{0a}}$ (GeV)	$\Delta\sigma^{(1)}$ (pb)	$\sigma_{t\bar{t}}^{(1)}$ (pb)	$\Delta\sigma^{(2)}$ (pb)	$\sigma_{t\bar{t}}^{(2)}$ (pb)	$\Delta\sigma^{(3)}$ (pb)	$\sigma_{t\bar{t}}^{(3)}$ (pb)
150	400	0.186	5.637	1.771	7.222	2.858	8.309
150	450	0.098	5.549	0.922	6.373	1.469	6.920
150	500	0.030	5.482	0.427	5.878	0.690	6.141
350	400	1.702	7.154	2.958	8.410	3.915	9.366
350	450	1.610	7.061	2.102	7.554	2.515	7.966
350	500	1.546	6.997	1.616	7.067	1.731	7.182

where Π stands for Π^0 , Π^{0a} , or Π_t^0 , and when B_1 and B_2 are gluons, the factors $S_{\Pi gg}$ in different cases are as follows.

For Π^0 and Π^{0a} with technifermion triangle loop [27],

$$S_{\Pi^0 g_b g_c}^{(Q)} = \frac{1}{\sqrt{3}} g_s^2 N_{\text{TC}} \delta_{bc}, \quad S_{\Pi^{0a} g_b g_c}^{(Q)} = \sqrt{2} g_s^2 N_{\text{TC}} d_{abc}. \quad (4)$$

For Π^0 and Π^{0a} with top-quark triangle loop [21],

$$S_{\Pi^0 g_b g_c}^{(t)} = \frac{C_t}{\sqrt{2}} g_s^2 J(R_{\Pi^0}) \delta_{bc},$$

$$S_{\Pi^{0a} g_b g_c}^{(t)} = \frac{C_t}{2} g_s^2 d_{abc} J(R_{\Pi^{0a}}), \quad (5)$$

with

$$J(R_{\Pi}) = -\frac{m_t'}{m_t} \frac{1}{R_{\Pi}^2} \int_0^1 \frac{dx}{x(1-x)} \ln[1 - R_{\Pi}^2 x(1-x)], \quad (6)$$

where $R_{\Pi} \equiv M_{\Pi}/m_t$.

The coupling of Π_t^0 to gluons via the top-quark triangle loop is isospin violating similar to the coupling of π^0 to gluons in the Gross-Treiman-Wilczek formula [22]. It can also be calculated from the formula in Ref. [21] which gives³

$$S_{\Pi_t^0 g_b g_c} = \frac{1}{\sqrt{2}} g_s^2 \delta_{bc} J(R_{\Pi_t^0}), \quad (7)$$

with

$$J(R_{\Pi_t^0}) = -\frac{m_t - m_t'}{m_t} \frac{1}{R_{\Pi_t^0}^2} \int_0^1 \frac{dx}{x(1-x)} \ln[1 - R_{\Pi_t^0}^2 x(1-x)], \quad (8)$$

where $R_{\Pi_t^0} \equiv M_{\Pi_t^0}/m_t$.

Finally the Π (Π^0 , Π^{0a} , or Π_t^0) propagator in Fig. 1 takes the form

$$\frac{i}{\hat{s} - M_{\Pi}^2 + iM_{\Pi}\Gamma_{\Pi}}, \quad (9)$$

where $\sqrt{\hat{s}}$ is the c.m. energy and Γ_{Π} is the total width of the PGB Π . The $iM_{\Pi}\Gamma_{\Pi}$ term in Eq. (11) is important when \hat{s} is close to M_{Π}^2 . The widths Γ_{Π^0} , $\Gamma_{\Pi^{0a}}$, and $\Gamma_{\Pi_t^0}$ can be obtained as follows.

From Eqs. (1) and (4) we see that the dominant decay modes of Π^0 are $\Pi^0 \rightarrow b\bar{b}$ and $\Pi^0 \rightarrow gg$, so that

$$\Gamma_{\Pi^0} \approx \Gamma(\Pi^0 \rightarrow b\bar{b}) + \Gamma(\Pi^0 \rightarrow g_a g_b). \quad (10)$$

From Eqs. (1) and (5), we can obtain

$$\Gamma(\Pi^0 \rightarrow b\bar{b}) = \frac{3C_b^2 m_b'^2 M_{\Pi}}{16\pi F^2} \sqrt{1 - \frac{4m_b^2}{M_{\Pi}^2}} \quad (11)$$

and

$$\Gamma(\Pi^0 \rightarrow g_a g_b) = \alpha_s^2 N_{\text{TC}}^2 \frac{1}{96\pi^3} \frac{M_{\Pi}^3}{F^2} \left| 1 + \frac{\sqrt{6} C_t J(R_{\Pi^0})}{2N_{\text{TC}}} \right|^2. \quad (12)$$

It has been shown [21,28] that Π^{0a} decays dominantly into $t\bar{t}$, gg , and gZ , so that

$$\Gamma_{\Pi^{0a}} \approx \Gamma(\Pi^{0a} \rightarrow b\bar{b}) + \Gamma(\Pi^{0a} \rightarrow g_a g_b) + \Gamma(\Pi^{0a} \rightarrow t\bar{t}) + \Gamma(\Pi^{0a} \rightarrow gZ). \quad (13)$$

From Eqs. (1) and (4) and the value of $S_{\Pi^{0a} gZ}$ given in Refs. [25,17], we can obtain

$$\Gamma(\Pi^{0a} \rightarrow q\bar{q}) = \frac{C_q^2 m_q'^2 M_{\Pi^{0a}}}{16\pi F^2} \sqrt{1 - \frac{4m_q^2}{M_{\Pi^{0a}}^2}}, \quad q=t, b, \quad (14)$$

³It is proportional to the isospin-violating factor $(m_t - m_b)/(m_t + m_b) \approx 1$.

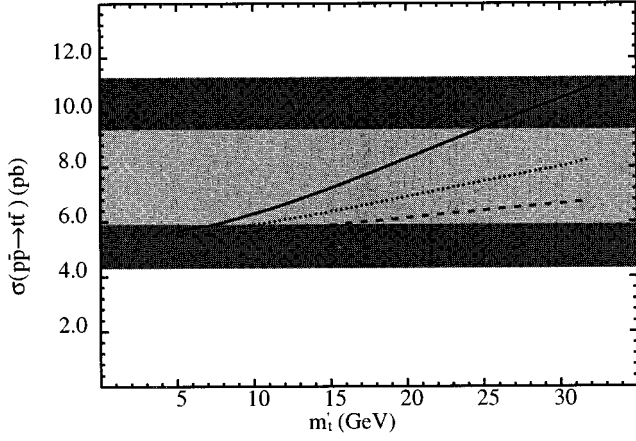


FIG. 2. The plot of $\sigma_{t\bar{t}}$ versus $m'_{t\bar{t}}$ for $m_{\Pi^0} = 150$ GeV at the Tevatron. The solid, dashed, and dotted lines stand for $m_{\Pi^0a} = 400, 450,$ and 500 GeV, respectively. The CDF data are indicated by the shaded band.

$$\Gamma(\Pi^{0a} \rightarrow g_a g_b) = \Gamma^{(\mathcal{Q})}(\Pi^{0a} \rightarrow g_a g_b) \left| 1 + \frac{C_r J(R_{\Pi^{0a}})}{2\sqrt{2}N_{\text{TC}}} \right|^2$$

$$= \frac{5\alpha_s^2 N_{\text{TC}}^2}{384\pi^3} \frac{M_{\Pi^{0a}}^3}{F^2} \left| 1 + \frac{C_r J(R_{\Pi^{0a}})}{2\sqrt{2}N_{\text{TC}}} \right|^2, \quad (15)$$

$$\Gamma(\Pi^{0a} \rightarrow gZ) = \frac{\alpha\alpha_s}{144\pi^3} \left(\frac{N_{\text{TC}}}{4} \right)^2 \tan^2 \theta_w \frac{M_{\Pi^{0a}}^3}{F^2}. \quad (16)$$

Since the top-pion mass is around 200 GeV, it decays mainly into gg . Thus from Eq. (3) we obtain

$$\Gamma_{\Pi_t^0} \approx \Gamma(\Pi_t^0 \rightarrow g_a g_b) = \frac{\alpha_s^2}{64\pi^3} \frac{M_{\Pi_t^0}^3}{F_t^2} |J(R_{\Pi_t^0})|^2. \quad (17)$$

With the above formulas, we can obtain the production amplitudes given in the Appendix.

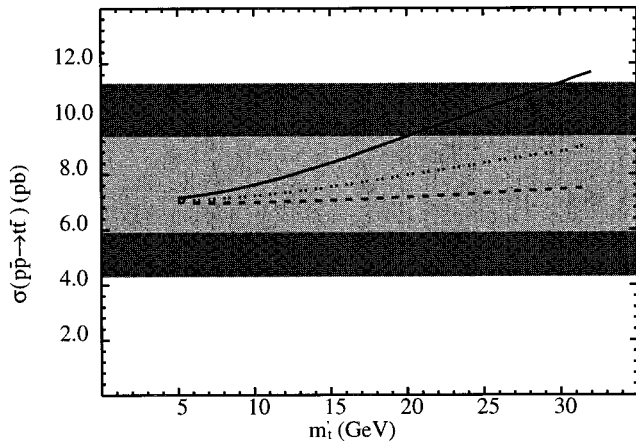


FIG. 3. Same as Fig. 2 but for $m_{\Pi^0} = 350$ GeV.

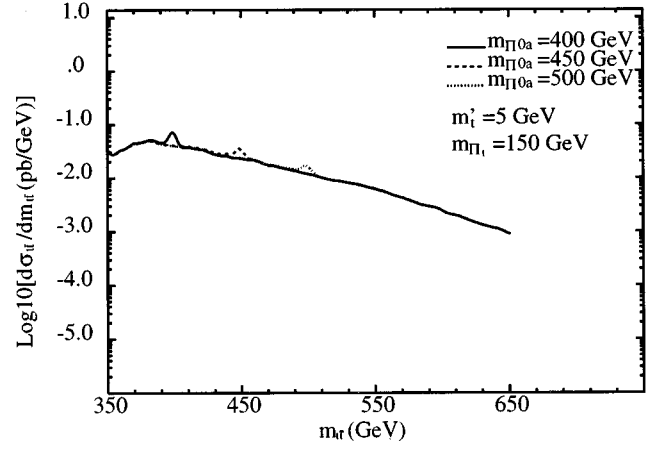


FIG. 4. Differential cross section $d\sigma_{t\bar{t}}/dm_{t\bar{t}}$ (in a logarithmic scale) versus the $t\bar{t}$ invariant mass $m_{t\bar{t}}$ at the Tevatron for $m_{\Pi^0a} = 400, 450,$ and 500 GeV with $m_{\Pi^0} = 150$ GeV, $m'_t = 5$ GeV, and $m_{\Pi_t} = 150$ GeV.

III. $t\bar{t}$ PRODUCTION CROSS SECTIONS AT THE TEVATRON AND THE LHC

Once we have the cross section at the parton level $\hat{\sigma}$, the cross section at the hadron collider is obtained by convoluting it with the parton distributions [29]

$$\sigma(pp(\bar{p}) \rightarrow t\bar{t}) = \sum_{ij} \int dx_i dx_j f_i^{(p)}(x_i, Q) f_j^{(p(\bar{p}))}(x_j, Q)$$

$$\times \hat{\sigma}(ij \rightarrow t\bar{t}), \quad (18)$$

where i and j stand for the partons $g, q,$ and \bar{q} ; x_i is the fraction of the longitudinal momentum of the proton (antiproton) carried by the i th parton; $Q^2 \approx \hat{s}$; and $f_i^{(p(\bar{p}))}$ is the parton distribution functions in the proton (antiproton). In this paper, we take the MRS set A' parton distribution for $f_i^{(p(\bar{p}))}$. Taking into account of the QCD corrections, we shall multiply the obtained σ by a factor 1.6 [3] as what was done

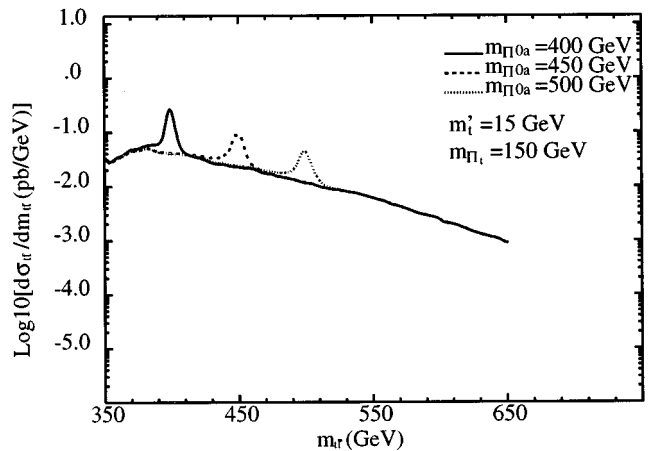


FIG. 5. Same as Fig. 4 but with $m'_t = 15$ GeV and $m_{\Pi^0} = 150$ GeV.

TABLE II. $t\bar{t}$ production cross section $\sigma(gg \rightarrow \Pi^{0(a)}(\Pi^0, \Pi_t^0) \rightarrow t\bar{t})$ at the $\sqrt{s}=14$ TeV LHC in the top-color-assisted multiscale walking technicolor model with $m_{\Pi^0}=150$ GeV. $\Delta\sigma^{(i)}$ is the TOPCMTC correction to the tree-level SM cross section and $\sigma_{t\bar{t}}^{(i)}$ is the total cross section, where $i=1,2$ correspond to $m_t'=5$ GeV and 15 GeV, respectively. A factor of 1.6 of QCD corrections has been taken into account.

$M_{\Pi_t^0}$ (GeV)	$M_{\Pi^{0a}}$ (GeV)	$\Delta\sigma^{(1)}$ (nb)	$\sigma_{t\bar{t}}^{(1)}$ (nb)	$\Delta\sigma^{(2)}$ (nb)	$\sigma_{t\bar{t}}^{(2)}$ (nb)
150	400	0.123	0.911	1.512	2.301
150	450	0.116	0.905	1.264	2.053
150	500	0.084	0.872	0.947	1.736
350	400	1.022	1.811	2.213	3.002
350	450	1.024	1.813	1.958	2.747
350	500	0.998	1.787	1.650	2.438

in Ref. [18]⁴.

The main purpose of Ref. [18] is to show the signal of Π^{0a} at the Tevatron, so that they only calculated the technifermion-loop contributions and neglected the interference between $\mathcal{A}_{\text{tree}}^{\text{SM}}(gg \rightarrow t\bar{t})$ and $\mathcal{A}(g_b g_c \rightarrow \Pi^{0a} \rightarrow t\bar{t})$ as a first investigation. In this section, we present the cross sections at the Tevatron and the LHC in TOPCMTC models considering the contributions of Π^{0a} , Π^0 , and Π_t^0 from Fig. 1(a) and Fig. 1(b) with the interferences taken into account. In our calculation, we take the more updated parton distribution functions MRS set A' instead of Eichten-Hinchliffe-Lane-Quigg (EHLQ) set 1 taken in Ref. [18]. The fundamental SM parameters in our calculation are taken to be $m_t=176$ GeV, $\sin^2\theta_W=0.231$, and $\alpha_s(\sqrt{s})$, the same as that in the MRS set A' parton distributions. For the parameters in the TOPCMTC models, we simply take $C_t=C_b=1$ and $m_b'=m_b=4.9$ GeV and take the reasonable values $F=40$ GeV and $F_t=50$ GeV in this calculation. For the technipion masses, we fix $M_{\Pi^0}=150$ GeV, and vary $M_{\Pi^{0a}}$ from 400 GeV to 500 GeV. The values of Π_t^0 and m_t' depend on the parameters in the TOPCMTC models. To see how these val-

ues affect the cross sections, we take some reasonable values for each of them, namely, $M_{\Pi_t^0}=150$ GeV and 350 GeV, $m_t'=5, 15$, and 20 GeV.

The results of the cross sections at the 1.8 TeV Tevatron are listed in Table I, in which $\Delta\sigma_{t\bar{t}}^{(i)}$ is the TOPCMTC correction (including the interferences between the TOPCMTC amplitudes and the tree-level SM amplitudes) to the tree-level SM cross section in the total cross section $\sigma_{t\bar{t}}^{(i)}$, with $i=1,2,3$ corresponding to $m_t'=5$ GeV, 15 GeV, and 20 GeV. We see that for most values of the parameters the cross sections $\sigma_{t\bar{t}}$ are consistent with the new CDF data. Therefore the CDF data give constraints on the values of $m_{\Pi^{0a}}$ and m_t' which depend on the specific model. To see the constraints more precisely, we plot the cross section versus m_t' in Fig. 2 (with $m_{\Pi^0}=150$ GeV) and Fig. 3 (with $m_{\Pi_t^0}=350$ GeV), in which the solid, dashed, and dotted lines stand for $m_{\Pi^{0a}}=400, 450$, and 500 GeV, respectively. Comparing with the new CDF data (the two shaded bands corresponding to 1σ and 2σ errors, respectively), we see that there are parameter ranges outside the bands of the CDF data, especially for $m_{\Pi_t^0}=150$ GeV, and the range of parameters $m_{\Pi^{0a}}=400$ GeV with $m_t'>25$ GeV is disfavored at the 1σ level; for $m_{\Pi_t^0}=350$ GeV, the range of parameters $m_{\Pi^{0a}}=400$ GeV with all $m_t'>20$ GeV is disfavored at the 1σ level and $m_t'>30$ GeV is disfavored at the 2σ level.

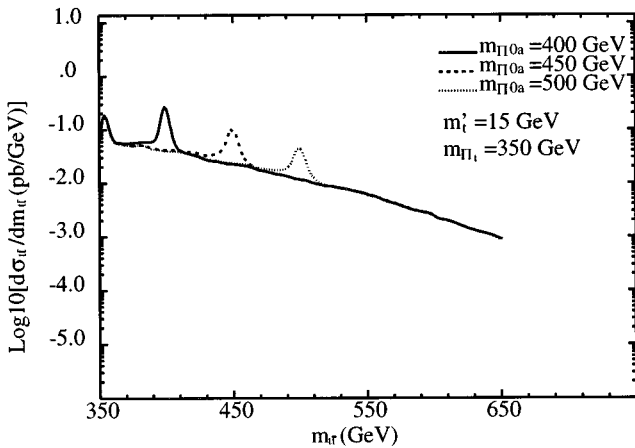


FIG. 6. Same as Fig. 4 but with $m_t'=15$ GeV and $m_{\Pi_t^0}=350$ GeV.

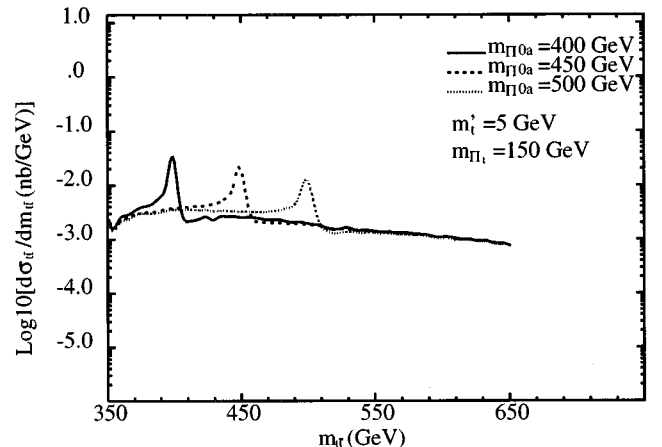


FIG. 7. Same as Fig. 4 but at the LHC.

⁴Since our tree-level result for $\sqrt{s}=1.8$ TeV is 3.41 pb, we multiply the obtained σ by $1.6\sim 5.5/3.4$ instead of 1.5 as what is used in Ref. [18].

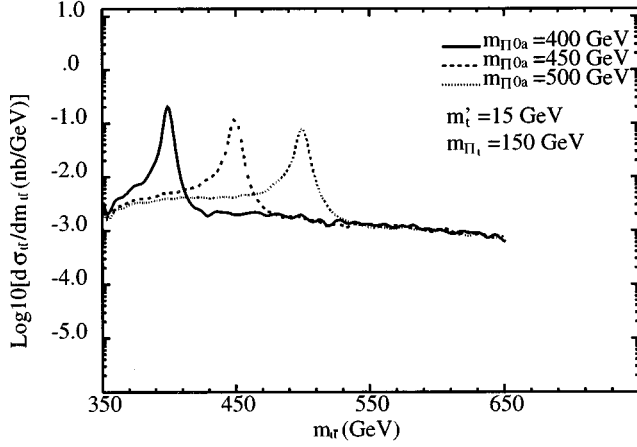


FIG. 8. Same as Fig. 5 but at the LHC.

In Figs. 4–6, we plot the differential cross sections $d\sigma_{t\bar{t}}/dm_{t\bar{t}}$ versus the $t\bar{t}$ invariant mass $m_{t\bar{t}}$ at the $\sqrt{s}=1.8\text{TeV}$ Tevatron for various values of the parameters. We see that the peak of the Π^{0a} resonance emerges when $m_{\Pi^{0a}}$ lies in the range of 400–500 GeV. For the case of $m_{\Pi^0}=350$ GeV, the Π_t^0 peak can also be seen. Assuming an integrated luminosity of $1fb^{-1}$ and 10% detecting efficiency for $t\bar{t}$, we find that the SM backgrounds in 50 GeV bin of the continuous production $p\bar{p}\rightarrow q\bar{q}\rightarrow t\bar{t}$ are about 52, 120, 75, and 39 events for $m_{t\bar{t}}=350$ GeV, 400 GeV, 450 GeV, and 500 GeV, respectively. The peaks in Fig. 4 have so small statistical significancies of S/\sqrt{B} that they can not be observed. In Figs. 5 and 6 the S/\sqrt{B} ratios corresponding to $m_{\Pi^{0a}}=400$ GeV, 450 GeV, and 500 GeV are about 9, 7, and 4. So the peaks are observable from the backgrounds. The Π^{0t} peak in Fig. 6 has $S/\sqrt{B}\sim 10$. It is also observable. Thus the model can be tested by the differential cross section for certain values of the parameters as long as the assumed integrated luminosity can be reached.

In Table II, we list the values of $\Delta\sigma_{t\bar{t}}$ and $\sigma_{t\bar{t}}$ at the $\sqrt{s}=14$ TeV LHC. We see that the cross sections are much larger than those at the Tevatron due to the fact that at the LHC $t\bar{t}$ production is dominated by gluon fusion. The obtained cross section is significantly larger than the SM predicted value, so that it can be easily tested by the future experiment. In Figs. 7–9, we plot the differential cross sections at the LHC for various values of the parameters. We see that differential cross sections are similar to those at the Tevatron but the peaks are more significant due to the same reason. All the peaks have very large S/\sqrt{B} ratios with the integrated luminosity of 10^5pb^{-1} and $t\bar{t}$ detecting efficiency of 10% so that the models can be better tested at the LHC.

APPENDIX

Here we present the production amplitudes needed in the text. They are

$$\begin{aligned} \mathcal{A}(g_b g_c \rightarrow \Pi^{0a} \rightarrow t\bar{t}) &= \mathcal{A}^{(Q)}(g_b g_c \rightarrow \Pi^{0a} \rightarrow t\bar{t}) + \mathcal{A}^{(t)}(g_b g_c \rightarrow \Pi^{0a} \rightarrow t\bar{t}) \\ &= \frac{C_t m'_t g_s^2 [N_{\text{TC}} + C_r J(R_{\Pi^{0a}})/(2\sqrt{2})] d_{abc}}{4\pi^2 \sqrt{2} F^2 [\hat{s} - M_{\Pi^{0a}} + iM_{\Pi^{0a}}\Gamma_{\Pi^{0a}}]} \left(\bar{t} \gamma_5 \frac{\lambda^a}{2} t \right) \epsilon_{\mu\nu\lambda\rho} k_1^\mu k_2^\rho \epsilon_1^\nu \epsilon_2^\lambda, \end{aligned} \quad (\text{A1})$$

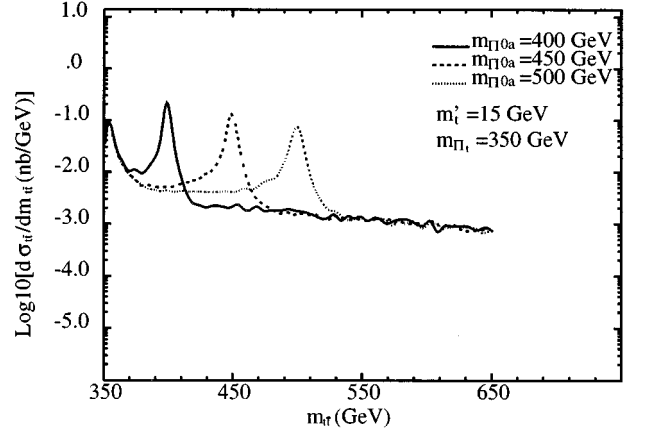


FIG. 9. Same as Fig. 6 but at the LHC.

IV. CONCLUSIONS

In this paper, we studied the $t\bar{t}$ production cross sections at the $\sqrt{s}=1.8$ TeV Tevatron and the $\sqrt{s}=14$ TeV LHC in the TOPCMTC models. The TOPCMTC contributions are mainly via the s -channel PGB's Π^{0a} , Π^0 , and Π_t^0 through gluon fusion. We calculated both the diagrams in Figs. 1(a) and 1(b), and took into account the interferences between the tree-level SM amplitudes and the TOPCMTC amplitudes. The MRS set A' parton distribution functions are taken in this calculation. In the study, we take $m_{\Pi^0}=150$ GeV and vary other parameters in the models. Our results show that the production cross sections are enhanced by the TOPCMTC contributions. With the reasonable parameters, the production cross sections are consistent with the experimental data. The present CDF datum on the production cross section gives constraints on the model-dependent parameters $m_{\Pi^{0a}}$ and m'_t ; i.e., $m_{\Pi^{0a}}=400$ GeV with large m'_t is disfavored. In the differential cross sections, clear peaks of the Π^{0a} and Π_t^0 can be seen for reasonable range of the parameters, so that the models are experimentally testable at the Tevatron and the LHC. The cross section at the LHC is significantly larger than the SM predicted value, and the peaks are more significant at the LHC than at the Tevatron due to the fact that $t\bar{t}$ production at the LHC is dominated by gluon fusion. Therefore the models can be better tested at the LHC.

ACKNOWLEDGMENTS

C.-X.Y. would like to thank B.-L. Young for his valuable discussions. This work was supported by National Natural Science Foundation of China, the Natural Foundation of Henan Scientific Committee, and the Fundamental Research Foundation of Tsinghua University.

$$\begin{aligned} \mathcal{A}(g_b g_c \rightarrow \Pi^0 \rightarrow t\bar{t}) &= \mathcal{A}^{(0)}(g_b g_c \rightarrow \Pi^0 \rightarrow t\bar{t}) + \mathcal{A}^{(t)}(g_b g_c \rightarrow \Pi^0 \rightarrow t\bar{t}) \\ &= \frac{C_t m'_t g_s^2 [N_{TC} + \sqrt{6} C_t J(R_{\Pi^0})/2] \delta_{bc}}{8\pi^2 \sqrt{6} F^2 [\hat{s} - M_{\Pi^0} + i M_{\Pi^0} \Gamma_{\Pi^0}]} (\bar{t} \gamma_5 t) \epsilon_{\mu\nu\lambda\rho} k_1^\mu k_2^\rho \epsilon_1^\nu \epsilon_2^\lambda, \end{aligned} \quad (\text{A2})$$

and

$$\mathcal{A}(g_b g_c \rightarrow \Pi_t^0 \rightarrow t\bar{t}) = \frac{(m_t - m'_t) g_s^2 J(R_{\Pi_t^0}) \delta_{bc}}{16\pi^2 F_t^2 [\hat{s} - M_{\Pi_t^0}^2 + i M_{\Pi_t^0} \Gamma_{\Pi_t^0}]} (\bar{t} \gamma_5 t) \epsilon_{\mu\nu\lambda\rho} k_1^\mu k_2^\rho \epsilon_1^\nu \epsilon_2^\lambda. \quad (\text{A3})$$

It is easy to obtain the SM tree-level $t\bar{t}$ production amplitudes

$$\mathcal{A}_{\text{tree}}^{\text{SM}}(q\bar{q} \rightarrow t\bar{t}) = \frac{i g_s^2 \bar{v}(p_{\bar{q}}) \gamma^\mu (\lambda^a/2) u(p_q) \bar{u}(p_t) \gamma_\mu (\lambda^a/2) v(p_{\bar{t}})}{\hat{s}} \quad (\text{A4})$$

and

$$\mathcal{A}_{\text{tree}}^{\text{SM}}(gg \rightarrow t\bar{t}) = \mathcal{A}_{\text{tree}}^{\text{SM}(s)}(gg \rightarrow t\bar{t}) + \mathcal{A}_{\text{tree}}^{\text{SM}(t)}(gg \rightarrow t\bar{t}) + \mathcal{A}_{\text{tree}}^{\text{SM}(u)}(gg \rightarrow t\bar{t}), \quad (\text{A5})$$

with

$$\mathcal{A}_{\text{tree}}^{\text{SM}(s)}(gg \rightarrow t\bar{t}) = -i g_s^2 [(k_2 - k_1)^\mu (\epsilon_2 \cdot \epsilon_1) + (k_2 + 2k_1) \cdot \epsilon_2 \epsilon_1^\mu - (2k_2 + k_1) \cdot \epsilon_1 \epsilon_2^\mu] \frac{1}{\hat{s}} \bar{u}(p_t) \gamma_\mu \left(i f_{abc} \frac{\lambda^c}{2} \right) v(p_{\bar{t}}), \quad (\text{A6})$$

$$\mathcal{A}_{\text{tree}}^{\text{SM}(t)}(gg \rightarrow t\bar{t}) = -i g_s^2 \frac{\bar{u}(p_t) \not{\epsilon}_1 (\not{q} - m_t) \not{\epsilon}_2 (\lambda^b/2) (\lambda^a/2) v(p_{\bar{t}})}{q^2 - m_t^2}, \quad q \equiv p_t - k_1, \quad (\text{A7})$$

$$\mathcal{A}_{\text{tree}}^{\text{SM}(u)}(gg \rightarrow t\bar{t}) = \mathcal{A}_{\text{tree}}^{\text{SM}(t)}(gg \rightarrow t\bar{t}) [1 \leftrightarrow 2, a \leftrightarrow b], \quad (\text{A8})$$

where k_1, k_2 are the momenta of the two initial-state gluons and p_t is the momentum of the top quark.

Adding all the $q\bar{q} \rightarrow t\bar{t}$ and $gg \rightarrow t\bar{t}$ amplitudes, respectively, we obtain the total $t\bar{t}$ production amplitude.

- [1] G. F. Tartarelli, Fermilab Report No. CDF/PUB/ TOP/PUBLIC/3664, 1996 (unpublished).
- [2] CDF Collaboration, F. Abe *et al.*, Phys. Rev. Lett. **74**, 2626 (1995); D0 Collaboration, S. Abachi *et al.*, *ibid.* **74**, 2632 (1995).
- [3] E. Laenen, J. Smith, and W. L. van Neerven, Phys. Lett. B **321**, 254 (1994); E. L. Berger and H. Contopanagos, in *Proceedings of the International Symposium on Heavy Flavor and Electroweak Theory*, Beijing, China, 1995, edited by C. H. Chang and C. S. Huang (World Scientific, Singapore, 1995), pp. 25–36.
- [4] S. Weinberg, Phys. Rev. D **13**, 974 (1976); **19**, 1277 (1979); L. Susskind, *ibid.* **20**, 2619 (1979).
- [5] S. Dimopoulos and L. Susskind, Nucl. Phys. **B155**, 237 (1979); E. Eichten and K. Lane, Phys. Lett. **90B**, 125 (1980).
- [6] B. Holdom, Phys. Rev. D **24**, 1441 (1981); Phys. Lett. **150B**, 301 (1985); T. Appelquist, D. Karabali, and L. C. R. Wijewardhana, Phys. Rev. Lett. **57**, 957 (1986).
- [7] T. Appelquist and G. Triantaphyllou, Phys. Lett. B **278**, 345 (1992); R. Sundrum and S. Hsu, Nucl. Phys. **B391**, 127 (1993); T. Appelquist and J. Terning, Phys. Lett. B **315**, 139 (1993).
- [8] K. Lane and E. Eichten, Phys. Lett. B **222**, 274 (1989); K. Lane and M. V. Ramana, Phys. Rev. D **44**, 2678 (1991).
- [9] R. S. Chivukula, B. A. Dobrescu, and J. Terning, Proceedings of the International Workshop on Particle Theory and Phenomenology, Ames, Iowa, 1995, Report No. BUHEP-95-22, hep/9506450 (unpublished).
- [10] T. Appelquist *et al.*, Phys. Lett. B **220**, 223 (1989); R. S. Chivukula, A. G. Gohen, and K. Lane, Nucl. Phys. **B343**, 554 (1990).
- [11] The LEP Collaborations ALEPH, DELPHI, L3, OPAL, and the LEP Electroweak Working Group, CERN Report No. CERN-PPE/95-172 (unpublished).
- [12] Chong-Xing Yue, Yu-Ping Kuang, and Gong-Ru Lu, J. Phys. G (to be published).
- [13] Guo-Hong Wu, Phys. Rev. Lett. **74**, 4137 (1995); Chong-Xing Yue, Yu-Ping Kuang, Gong-Ru Lu, and Ling-De Wan, Phys. Rev. D **52**, 5314 (1995).
- [14] C. T. Hill, Phys. Lett. B **266**, 419 (1991); S. P. Martin, Phys. Rev. D **45**, 4283 (1992); **46**, 2197 (1992); Nucl. Phys. **B398**, 359 (1993); M. Linder and D. Ross, Nucl. Phys. **B370**, 30 (1992); C. T. Hill, D. Kennedy, T. Onogi, and H. L. Yu, Phys. Rev. D **47**, 2940 (1993); W. A. Bardeen, C. T. Hill, and M. Lindner, *ibid.* **41**, 1649 (1990).
- [15] K. Lane, Phys. Lett. B **357**, 624 (1995).
- [16] C. T. Hill, Phys. Lett. B **345**, 483 (1995); K. Lane and E. Eichten, *ibid.* **352**, 382 (1995).

- [17] V. Lubicz, Nucl. Phys. **B404**, 559 (1993); V. Lubicz and P. Santorelli, *ibid.* **B460**, 3 (1996).
- [18] E. Eichten and K. Lane, Phys. Lett. B **327**, 129 (1994).
- [19] B. Holdom and M. V. Ramana, Phys. Lett. B **353**, 295 (1995).
- [20] G. L. Lu, Y. Hua, J. M. Yang, and X. L. Wang, Phys. Rev. D **54**, 1083 (1996).
- [21] D. Slaven, Bing-Ling Young, and Xin-Min Zhang, Phys. Rev. D **45**, 4349 (1992); Chong-Xing Yue, Xue-Lei Wang, and Gong-Ru Lu, J. Phys. G **19**, 821 (1993).
- [22] D. J. Gross, S. B. Treiman, and F. Wilczek, Phys. Rev. D **19**, 2188 (1979).
- [23] A. D. Martin, W. J. Stirling, and R. G. Roberts, Phys. Lett. B **354**, 155 (1995).
- [24] B. Balaji, Phys. Rev. D **53**, 1699 (1996).
- [25] L. Randall and E. H. Simmons, Nucl. Phys. **B380**, 3 (1992).
- [26] S. Adler, Phys. Rev. **177**, 2426 (1969); J. S. Bell and R. Jackiw, Nuovo Cimento A **60**, 47 (1969).
- [27] S. Dimopoulos, S. Raby, and G. L. Kane, Nucl. Phys. **B182**, 77 (1981); J. Ellis, *et al.*, *ibid.* **B182**, 529 (1981).
- [28] Chong-Xing Yue, Gong-Ru Lu, and Jin-Min Yang, Mod. Phys. Lett. A **8**, 2843 (1993).
- [29] E. Eichten, I. Hinchliffe, K. Lane, and C. Quigg, Rev. Mod. Phys. **56**, 579 (1984).